Photobleaching of Rhodamine 6G in Poly(vinyl alcohol) at the Ensemble and Single-Molecule Levels

Rob Zondervan, Florian Kulzer, Mikhail A. Kol'chenko, and Michel Orrit*

Molecular Nano-Optics and Spins (MoNOS), Leiden Institute of Physics (LION), Huygens Laboratory, Leiden University, P.O. Box 9504, 2300 RA Leiden, The Netherlands

Received: October 24, 2003

Photobleaching is a severely limiting factor in the optical study of single biomolecules. We investigate the photobleaching of rhodamine 6G (R6G) ensembles in poly(vinyl alcohol) (PVA) as a function of illumination time, excitation intensity, the presence of oxygen, and temperature. We observe nonexponential kinetics related to primary photobleaching through two dark states—the triplet state and a radical anion—and to secondary photobleaching after the optical excitation of those dark states. Reactions of the metastable states with oxygen can lead either to photoproducts or to a recovery of the ground state. Oxygen can therefore enhance or reduce photobleaching, depending on the experimental conditions. At low temperature, photobleaching is reduced although not completely suppressed. Despite the presence of the long-lived radical anion, we are able to observe single R6G molecules in PVA. At room temperature, only relatively bleaching-resistant molecules are resolved as individuals. At low temperature, the observation times become considerably longer. Our study shows that metastable states other than the triplet drastically affect photobleaching.

Introduction

Although hardly any biological molecule intrinsically fluoresces at convenient excitation wavelengths, a biomolecule can be labeled with fluorophore(s) in a controlled manner for optical investigation. The study of biomolecules has become an important application of single-molecule optics, especially at room temperature.[1−9] However, the time scales and the range of optical experiments on biological systems at room temperature are considerably limited by photobleaching. Bleaching is the irreversible conversion of a fluorescent molecule or particle into a nonfluorescent entity. In most cases, this process is photoinduced and hence is called photobleaching. Two circumstances make photobleaching especially detrimental to the optical study of single biomolecules. The first one is working at room temperature. Photobleaching efficiency increases with temperature because more reaction pathways become activated. The second one is the water or waterlike environment required by biomolecules. In aqueous solution, fluorophores are easily attacked by small reactive molecules such as oxygen or water itself.

The observation times in biological studies can be lengthened by removing oxygen with scavengers.[6,10] Another option is to use semiconductor quantum dots as labels for biomolecules[11,12] because they are generally more photostable than organic dyes and autofluorescent proteins.[13] Hydrophilic matrices other than water, for instance, the polymer poly(vinyl alcohol) (PVA) and sugars such as trehalose, have also been applied as matrices for experiments on single biomolecules.[14,15] These matrices have the advantage of allowing the incorporation of biomolecules into a rigid structure and in a less reactive environment than water. Nevertheless, the average observation time of single molecules in these matrices at room temperature,[15] 10 to 20 s, is still too short to study slow biological processes such as protein folding by following one and the same molecule over the full range of relevant time scales.[16] In this paper, we consider rhodamine 6G (R6G) in PVA as a model system to explore the photobleaching mechanisms in hydrophilic matrices.

The photobleaching mechanisms of organic dyes are complex and mostly unknown. They probably follow different pathways involving various intermediates. For instance, the photobleaching of Cy5 in water[17] involves at least three metastable intermediates. Some of these bleaching reactions need oxygen, and others require the optical excitation of an intermediate. It is therefore difficult to present a general description of photobleaching. A useful way to distinguish photobleaching pathways is to categorize them according to their dependence on experimental parameters. First of all, a given photobleaching pathway proceeds either by direct reaction from an excited state (singlet, triplet, or another metastable state) or by a "secondary", photoinduced reaction of one of these states, which thus requires the absorption of one or more additional laser photons. In principle, only the "primary" pathway should be observed at low enough intensities. However, the lifetime of dark states is sometimes so long that the two kinds of processes can be difficult to distinguish in practice. Another way to distinguish photobleaching mechanisms is to study the effect of the atmosphere and the temperature. The multiplicity of photobleaching mechanisms leads to a huge spread in the observation times of single molecules already at room temperature for different compounds and experimental conditions. To give an impression, the bleaching time can reach several hours for terrylene in *para*-terphenyl under an argon atmosphere,[18] but it does not exceed some hundreds of milliseconds for tetramethylrhodamine (TMR) attached to DNA at a surface.[19]

Primary Oxygen-Induced Photobleaching. At room temperature, oxygen is generally regarded as the most important reagent in photobleaching. Oxygen is believed to react in its singlet excited state, itself generated by reaction with the dye's triplet state. The oxidation mechanisms and products are poorly known. Recently, Christ et al.[18] have proposed that some of

* Corresponding author. E-mail: orrit@molphys.leidenuniv.nl.

10.1021/jp037222e CCC: $27.50
Published on Web 02/17/2004

the photooxidation products of single terrylene molecules are peroxides and diepoxides. In most single-molecule experiments in an air atmosphere, the observed photobleaching can be attributed to photooxidation reactions.[18−22] In ensemble studies, this is only the case at low dye concentrations (10^{-5} M and lower).[23−28] The diffusion constant and solubility of oxygen in the host matrix (resulting in the so-called permeability to oxygen) are important factors in the efficiency of photooxidation reactions. In the case of PVA, oxygen diffusion is enhanced when water is present in the polymer, softening its structure.[22,29] Because the temperature also affects the rigidity of the polymer, photobleaching can be applied as a probe for the glass transition, as was done for PVA ($T_g = 350$ K).[26,27,30]

Primary Photobleaching without Oxygen. Photooxidation is not the only primary photobleaching pathway because photobleaching is still observed in inert atmospheres,[21,31] in deoxygenated samples,[32] or when oxygen scavengers are added.[10] However, the characteristic bleaching times are about 1 to 2 orders of magnitude longer. This photobleaching pathway is believed to proceed through reactions of the triplet state with matrix molecules or with impurities other than oxygen. Such "non-oxygen-mediated" channels can become equally important as photooxidation and lead to complex bleaching behavior. This has been observed for ensembles[23−25,27,28] as well as for single molecules[33,34] of xanthene dyes such as fluorescein.

Photobleaching of Metastable States. Secondary photobleaching of metastable intermediates dominates the primary processes at high excitation intensities (higher than 1 MW/cm^2), where excitation of the excited singlet may also occur, but it can take place at much lower intensities for long-lived metastable states.[17] The highly excited states generated by secondary excitation are very reactive and are therefore particularly prone to photobleaching.[33,35] For the same reason, photobleaching is also enhanced by two-photon compared to one-photon excitation[36,37] or when the molecule sees a high infrared intensity, for example, in an optical trap.[38] However, as a further complication, the excitation of metastable states such as the triplet can repopulate the singlet state (e.g., by reverse intersystem crossing[39]), potentially leading to a reduction of photobleaching.

Photobleaching and Temperature. Lowering the temperature leads to a drastic decrease of photobleaching. Most photobleaching processes are chemical reactions that must overcome an activation barrier. The immobilization of reactive molecules such as water at lower temperatures can also further reduce photobleaching. Single terrylene molecules on a surface were shown to survive considerably longer below the freezing point of water.[40]

In a previous paper,[41] we have reported the emissivity of an ensemble of R6G molecules in PVA under optical excitation. We could distinguish two parts in the time decay: the faster component was reversible and related to the photoblinking of individual molecules. The second component was irreversible and related to photobleaching. We have identified the main transient species involved in the photoblinking as the radical anion of R6G, formed through the triplet. This metastable state must be considered in the discussion of the photobleaching of R6G in PVA. In this paper, we investigate the observed photobleaching kinetics as a function of time, intensity, temperature, and the presence of oxygen. We again work with an ensemble because it directly provides us with the overall photobleaching behavior, whereas a quantitative single-molecule study would require exhaustive statistics. We observe complex photobleaching behavior, which indeed involves the lowest triplet state and the radical anion of R6G. We extend our model of photoblinking to the photobleaching kinetics and obtain qualitative agreement with the data. We perform single-molecule measurements to compare qualitatively with the ensemble results. Single molecules can be observed despite the long-lived radical anion. The fluorescence dynamics of the single molecules are in good agreement with the ensemble results.

Experimental Section

The sample preparation has been described previously.[41] The concentration of R6G in the PVA films is 2.0×10^{-5} M in the ensemble experiments and 1.0×10^{-9} M in the single-molecule experiments. Fused-quartz substrates are used in the ensemble study because of their low fluorescence background, which allows us to observe the long-time "tail" of the photobleaching curves. Glass substrates suffice for the single-molecule experiments because of the confocal background suppression. For the single-molecule experiments, the 1 wt % PVA solution is "cleaned" by irradiation for a few hours with a 100-W xenon arc, the output of which is sent through a water filter to remove the deep ultraviolet and infrared parts. Furthermore, the single-molecule samples are dried overnight in a vacuum exsiccator. The excitation wavelength (continuous wave) is 514.5 nm in both experiments.

The ensemble experiments are performed at variable intensity (2.5 to 320 W/cm^2), atmosphere (nitrogen, helium or air), and temperature (10 K to 295 K) in a setup described elsewhere.[41] As in our photoblinking experiments,[41] we use a pinhole-array mask (prepared at the Laser Centre of Loughborough College) with 10×10 holes of diameter 40 μm to restrict the dimensions of the illuminated sample and to achieve a homogeneous excitation field over the studied area. To compare time traces recorded at different excitation intensities directly, we always normalize the measured fluorescence intensity to the excitation intensity. This normalized quantity is defined as the emissivity of the ensemble, which is in turn normalized to the emissivity of the given hole at 65 mW/cm^2 (to correct for slight differences in the area of the holes). To obtain the complete emissivity decay trace due to photobleaching at a given intensity, a trace with a high temporal resolution (1 to 100 ms, depending on the excitation intensity) and a short duration (up to 30 s after unblocking the laser) is combined with a low-resolution (2 s), long-time trace (30 to 5000−80 000 s after unblocking the laser).

The single-molecule experiments are performed at 295 K in air and nitrogen atmospheres and in liquid helium at 1.5 K with the home-built laser-scanning confocal microscope of reference 42. To the original setup, we have added an optical shutter (Uniblitz, Vincent Associates), a laser-line cleanup filter (Laser Components LCS10-515-F), a dichroic beam splitter (AHF Analyzentechnik HQ530LP) to separate the excitation and detection light, and in the detection path a spatial filter and a notch-filter centered on 514.5 nm (Kaiser Optical Systems HNPF-514.5). The detection and excitation are performed through an objective with a focal length of 2.45 mm and a numerical aperture of 0.9. The objective is placed in the cryostat, and its focal spot has a fwhm of approximately 600 nm.

The experiment is controlled by an ADWin-based system (Keithley Instruments), with which we can automatically position molecules in the excitation focus while minimizing their exposure to the laser before recording time traces. From such a time trace, we obtain the bleaching time (i.e., the time it takes for the molecule to bleach under a given intensity of continuous irradiation). The excitation intensities reported in this paper are free-space intensities, which are not corrected for the local field

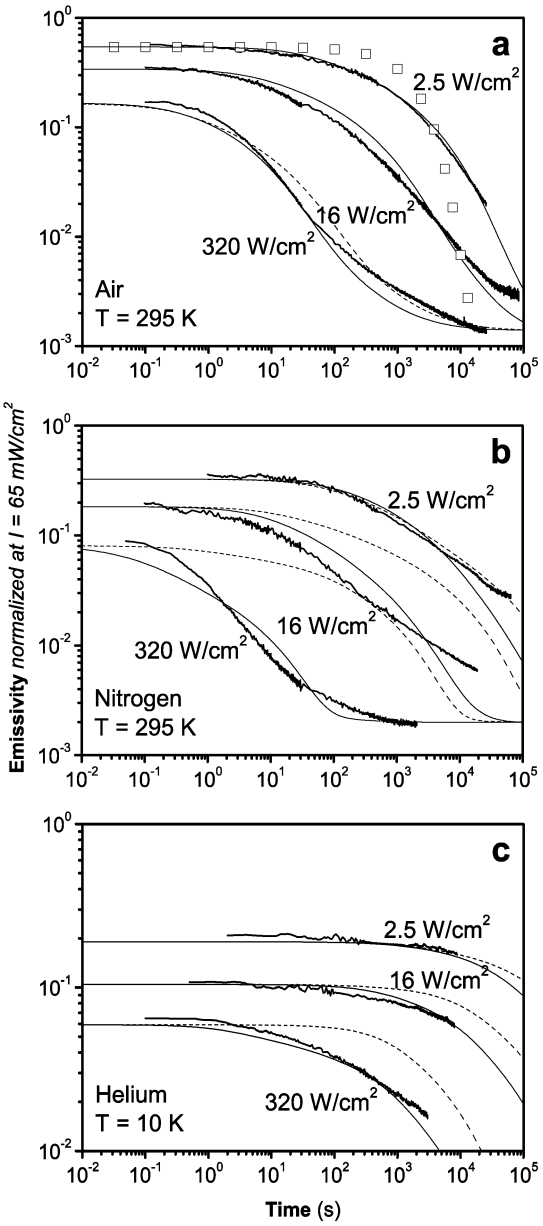

Figure 1. Emissivity decay traces due to photobleaching at three different excitation intensities: 2.5, 16, and 320 W/cm^2 in (a) air at 295 K, (b) nitrogen at 295 K, and (c) helium at 10 K. In plot a, the trace of open squares indicates a single exponential. Fits according to the model presented in Figure 6 and derived in the Appendix are indicated with dashed lines when they take only primary bleaching processes into account (b_1 and b_2) and with solid lines when they also take secondary bleaching processes through the excited states of D and T_1 (b_3 and b_4) into account. In plot a, the dashed and solid lines overlap for the two lower intensities, so only the solid line is visible.

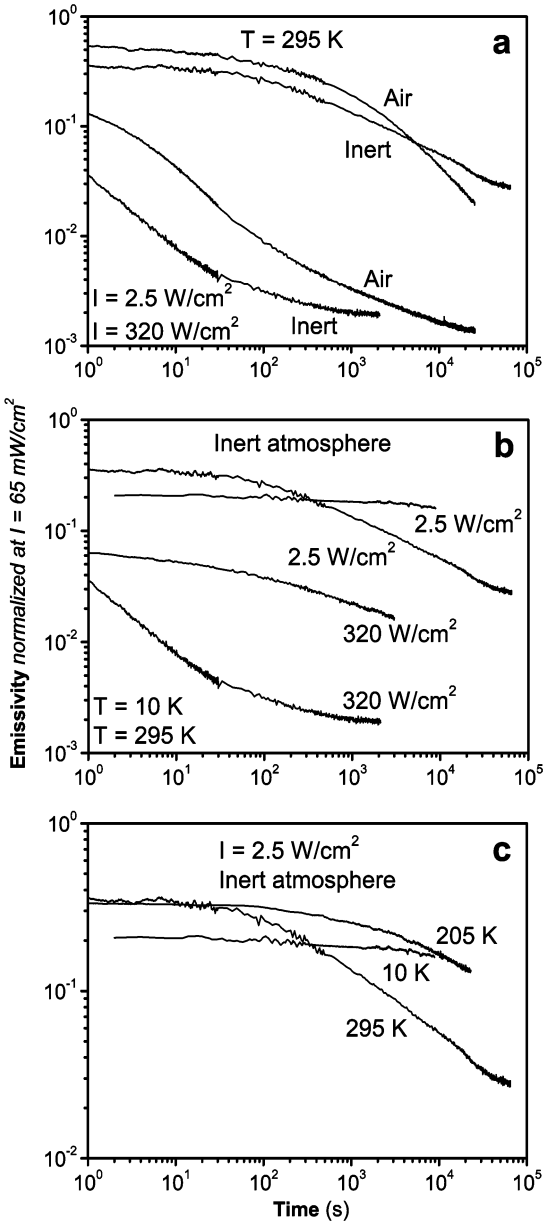

Figure 2. (a) Comparison of photobleaching time traces obtained in air or the inert atmosphere (nitrogen) at room temperature at 2.5 and 320 W/cm^2. (b) Photobleaching time traces obtained in the inert atmosphere at 295 and 10 K at 2.5 and 320 W/cm^2. (c) Variation of photobleaching with temperature for 2.5 W/cm^2. All traces, besides the one at 205 K (c), are also shown in Figure 1.

and index of refraction. Typical excitation intensities used in this work are 1.5 kW/cm^2 at room temperature and 0.4 kW/cm^2 in liquid helium. The images are recorded with higher intensities, up to 8 kW/cm^2 at room temperature. Because the single-molecule experiments are mainly meant as a comparison to the results of the ensemble experiments, only 40 to 100 bleaching events are acquired for each set of conditions.

Results

Ensemble Experiments. Figure 1 shows photobleaching traces recorded at three different excitation intensities in air and nitrogen at room temperature and in helium at 10 K. Figure 2 compares photobleaching time traces recorded in air and the inert atmosphere and traces at different temperatures. Both figures show that, as a result of photoblinking,[41] the initial emissivity level decreases with the intensity. All traces strongly deviate from single exponentials (cf. Figure 1a). Furthermore, the shape of the photobleaching traces clearly changes when the intensity increases (cf. Figure 1).

Figure 2a shows that photobleaching is more efficient in air than in the inert atmosphere at low intensity. This leads to a crossing of the curves. However, the same figure shows that the situation at high intensity is quite different. The bleaching curve in nitrogen stays below the one in air, at least during our observation time. This is a surprising result because it implies that photobleaching is more efficient in the inert atmosphere than in air at high intensity. However, the two high-intensity traces (cf. Figure 2a) come closer at longer times, which suggests

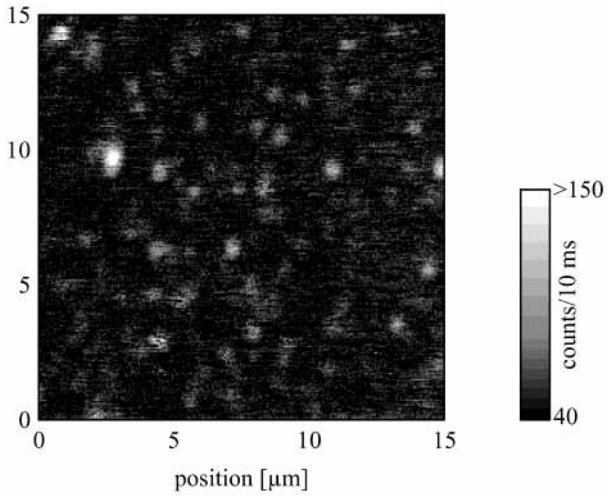

Figure 3. Confocally scanned fluorescence image ($15 \times 15\ \mu m^2$) of a poly(vinyl alcohol) film containing rhodamine 6G molecules measured at 1.5 K in liquid helium. The image consists of 256×256 points and is recorded with a time resolution of 10 ms/point at an intensity of 0.8 kW/cm^2. The sizes of the spots (about 600 nm) are limited by the optical quality of the objective in liquid helium. Most of them stem from single rhodamine 6G molecules.

that the most bleaching-resistant molecules are more stable in the inert atmosphere than in air.

Figure 2b shows the effect of temperature at low and high intensities. In our time window, at 10 K hardly any photobleaching is observed at 2.5 W/cm^2, which is clearly not the case at 320 W/cm^2, although the photobleaching is much reduced with respect to 295 K. Figure 2c shows that the most pronounced change takes place between 295 and 200 K. This is also observed at the higher excitation intensities (data not shown).

Single-Molecule Experiments. Figure 3 shows a typical example of a $15 \times 15\ \mu m^2$ fluorescence image generated by our setup at 1.5 K in liquid helium. From each spot in a given image, we can obtain a fluorescence time trace; a few examples are shown in Figure 4. Only the traces consisting of the contributions of one or two R6G molecules are used for further analysis. In this way, 89 time traces have been obtained at 295 K in air, 58 at 295 K in nitrogen, and 37 at 1.5 K in liquid helium. In these traces steplike bleaching behavior is observed, which confirms that the signal arose from single molecules. The time traces of very bright spots (cf. the top left corner of Figure 3) generally show multistep photobleaching, which indicates the presence of several molecules. Besides bleaching, blinking can be observed in the time traces. The off times can become very long, up to tens of seconds, as is visible in the lower trace of Figure 4b, for instance.

From every trace, the bleaching time of the molecules is determined. Two remarks about these times have to be made. First, the bleaching time, defined previously as the total duration of the time trace until bleaching, is not the same as the total time the molecule emits because of blinking. Second, we have to set a maximum waiting time to distinguish between bleaching and blinking with long off times. This procedure introduces some arbitrariness into the results. Figure 5 shows the histograms of the bleaching times obtained from the time traces recorded for the three different experimental conditions. The shape of the histograms differs significantly between room temperature and low temperature. At room temperature, the distributions of the bleaching times are fit reasonably well with a single-exponential, although a significant nonexponential tail is present (cf. insets in Figure 5a and b). The average bleaching time in air is roughly half as long as in the inert atmosphere, 11 versus 22 s. At low temperature, the histogram is completely different. The bleaching times are spread over orders of magnitude, and one-third of the molecules live longer than 1000 s. Some molecules were even found to bleach only after more than 1 h.

Discussion

Simulations of Ensemble Photobleaching. In the most naive model, photobleaching is a one-photon process with a constant quantum yield, β, in which the number of surviving molecules, N, decays exponentially with the number of absorbed photons, σQt:

$$N = N_0 \exp(-\beta\sigma Qt) \tag{1}$$

where σ is the absorption cross section of the dye and Q is the number of photons per unit time and unit area. The cross section σ is supposed to be independent of laser intensity as long as this intensity is much smaller than the saturation intensity of the three-level system including the triplet state. As pointed out in the Results section, the curves of Figure 1 immediately show that this single-exponential behavior can in no way describe the observed photobleaching. Furthermore, the strong dependence of the shape of the curves on intensity shows that photobleaching is not a function of the photon dose, Qt, only but that the cross section must depend on the excitation intensity already at weak intensities. This latter conclusion is not surprising because our study of photoblinking[41] has demonstrated the importance of two dark states (triplet and radical anion) in the photophysics of rhodamine dyes under illumination. These dark states deeply affect the photobleaching kinetics.

To understand the observed photobleaching curves (cf. Figures 1 and 2), we start from our photoblinking model for R6G in PVA.[41] Most of the molecules (about 95%, which we call population 1) quickly go from their triplet state to the radical

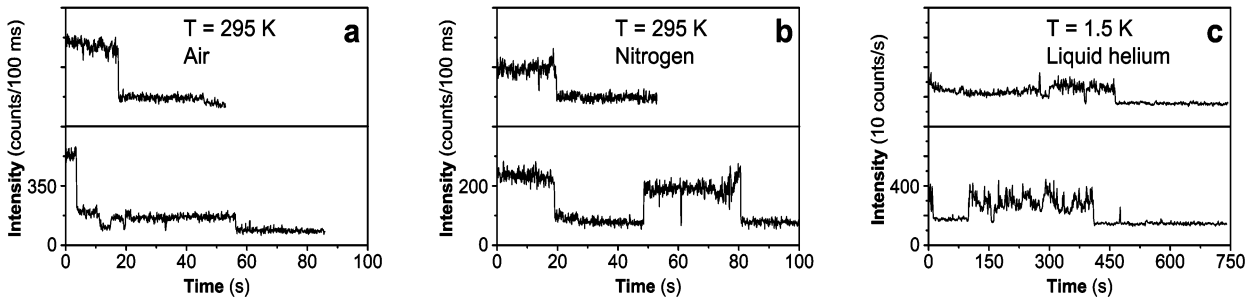

Figure 4. Examples of fluorescence time traces of single rhodamine 6G molecules in poly(vinyl alcohol) obtained in (a) air at 295 K, (b) nitrogen at 295 K, and (c) liquid helium at 1.5 K. The time resolution is 100 ms at 295 K and 1 s at 1.5 K, and the intensities are 1.5 kW/cm^2 at 295 K and 0.4 kW/cm^2 at 1.5 K. Some of the time traces show contributions of two molecules, such as the lower trace in plot a.

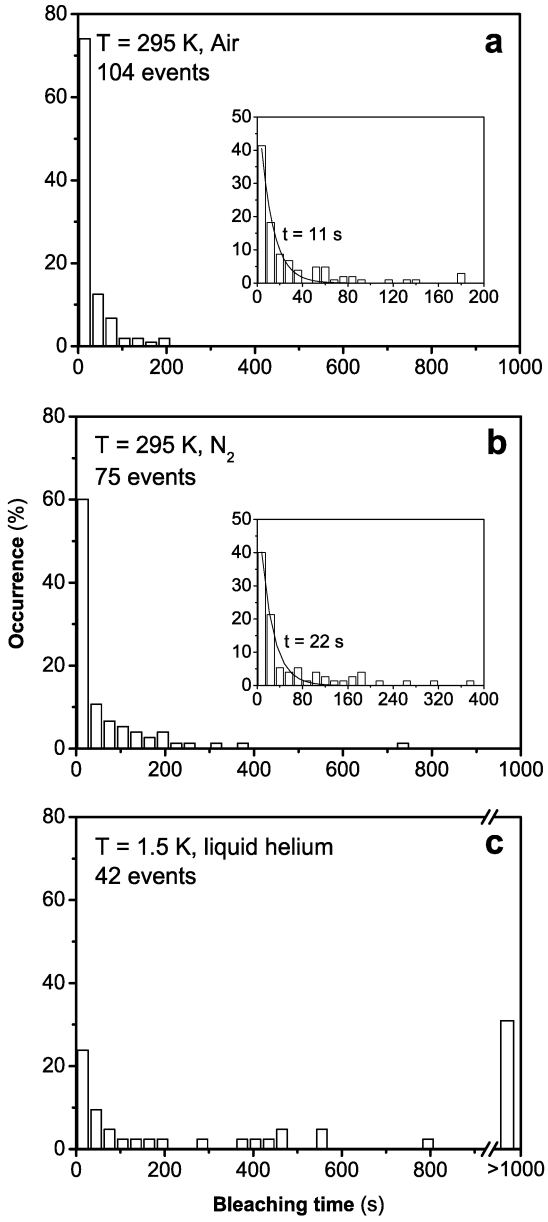

Figure 5. Histograms of bleaching times obtained in (a) air at 295 K at 1.5 kW/cm^2, (b) nitrogen at 295 K at 1.5 kW/cm^2, and (c) liquid helium at 1.5 K at 0.4 kW/cm^2. In each diagram, the total number of studied bleaching events is indicated. The insets in plots a and b show single-exponential fits of the respective distributions, yielding an average bleaching time of 11 s in air at 295 K and 22 s in nitrogen at 295 K. Note that for both histograms a significant nonexponential "tail" remains at longer times.

anion dark state, from where they return to the singlet ground state after a comparatively long radical lifetime (microseconds to seconds). The remaining molecules (approximately 5%, which we call population 2) do not form the radical anion but decay directly from the triplet state to the singlet ground state. These dark states must be reactive intermediates in photobleaching because if they were not they would "protect" the molecules from bleaching. In that case, photobleaching would saturate as soon as the dark states were populated, which happens at very low intensities.[41] The data of Figure 1 show that photobleaching does not saturate but proceeds at a lower and lower rate with time. Thus, we will have to introduce bleaching processes from the dark states.

Let us first consider that only primary bleaching of the excited states takes place. Any of the three excited states, S_1, T_1, D_0,

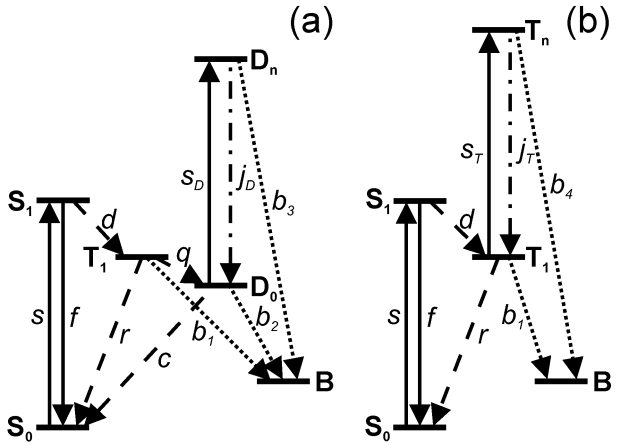

Figure 6. Schematic energy-level diagrams of (a) the six-level system describing the photobleaching of 95% of the rhodamine 6G (R6G) molecules in poly(vinyl alcohol) and (b) the five-level system describing the photobleaching of the remaining 5% of the R6G molecules. Both schemes include the electronic ground state (S_0), the first excited singlet state (S_1), the lowest triplet state (T_1), and the bleached "state" (B). In addition, part a contains the radical anion of R6G in the ground state (D_0) and in an excited state (D_n), and part b contains an excited triplet state (T_n) of R6G. Solid arrows indicate radiative transitions; dashed arrows, blinking transitions; dotted arrows, bleaching reactions; and dashed−dotted arrows, internal conversion.

can in principle be involved. (S_0 is assumed to be stable in the absence of light, i.e., no bleaching is observed in the dark.) Introducing bleaching rates from $S_1(b_0)$, $T_1(b_1)$, and $D_0(b_2)$ as fitting parameters, we obtain the dashed curves in Figure 1. In the actual fitting procedure (cf. Appendix), b_0 cannot be fit independently from b_1 and b_2. Therefore, we have neglected b_0 for the sake of simplicity. We have applied the known literature value for the bleaching quantum yield of R6G in aerated ethanol at low intensity[43] to describe the photobleaching of population 2. Moreover, we have distributed the bleaching rates (cf. Appendix) to better account for the strong nonexponential character of the observed photobleaching curves (cf. Figure 1). The dashed curves simulate the photobleaching in air at room temperature satisfactorily (Figure 1a), but when we apply this model to high intensities either in the inert atmosphere (Figure 1b) or at low temperatures (Figure 1c), the simulation is very poor.

Photobleaching is obviously accelerated with intensity, and we have to introduce secondary processes. In other words, we assume that the molecules of population 1 can be excited from D_0 to a higher excited state D_n of the radical, from which they bleach at a rate of b_3. We also have to introduce such a bleaching channel for population 2 (5% of the molecules with only the triplet as a dark state), with associated rate b_4, to simulate the bleaching behavior at longer times. From the literature,[44,45] we have indications that both dark states indeed absorb at 514.5 nm. The complete model describing the photobleaching of both populations, 1 and 2, is shown in Figure 6. This model fits all photobleaching curves in a qualitative way. Note, however, that the shape of the fitted curves differs from that of the data, which may indicate that our logarithmic distributions (cf. Appendix) are not correct or that our model is still incomplete (i.e., that more mechanisms and/or more intermediate levels should be considered). Our point here, however, is not to describe bleaching quantitatively but rather to propose and discuss plausible mechanisms for the main dependence of bleaching on the intensity, atmosphere, and temperature.

Nonexponential Photobleaching Kinetics. The observed nonexponential kinetics of all distinguishable photobleaching

processes (primary bleaching and secondary photobleaching of dark states of the molecules in population 1 and 2, cf. Table 1 in the Appendix) may be related to the many different reaction pathways probably contributing to each process. Comparable experiments on fluorescein[23−28] also revealed nonexponential photobleaching dynamics, although the triplet was supposed to be the only reactive metastable state. In one of their papers, Talhavini and Atvars[26] fit the photobleaching of fluorescein at a comparable concentration in PVA with a single rate. However, their experiments have a limited dynamical range, which makes it difficult to discern nonexponential behavior.

On the grounds of our simulations, it is impossible to determine which population (1 or 2) contributes to the tails of the bleaching curves (cf. Figures 1 and 2).

Photobleaching and Excitation. The change in the shape of the photobleaching curves, correctly reproduced by our model, is caused on one hand by the saturation of the radical population at low intensity[41] and on the other hand by the secondary photobleaching of this radical anion (and, less importantly, of the triplet state). Normally, secondary photobleaching of intermediate states is significant only at very high excitation intensities.[33,35] However, because the radical anion has a much longer lifetime than the triplet states, secondary photobleaching of the radical becomes significant at 2.5 W/cm^2 (at least in the inert atmosphere). The secondary photobleaching of the triplet for population 2 mainly takes place at times longer than minutes, when the molecules have absorbed a comparable number of photons as in high-power but short-time experiments.[33,35]

Photobleaching and the Atmosphere. The primary bleaching from both dark states (triplet and radical anion) is, as expected, enhanced by oxygen (cf. Table 1 in the Appendix). However, the secondary photobleaching from both dark states is so much reduced in air that it becomes negligible. This reduction leads to the paradoxical observation that at high intensity, photobleaching is much faster in the inert atmosphere than in air (cf. Figure 2a)! At first sight, the reduction seems to be the effect of the shortened lifetime in air of both the radical anion,[41] by 1 order of magnitude, and of the triplet state,[44,46] by 2 orders of magnitude. For the triplet photobleaching, this shortening indeed explains the observed decrease. However, this is not the case for the radical photobleaching, which is reduced by almost 3 orders of magnitude between inert and air atmospheres (cf. Table 1 in the Appendix). Because the bleaching rate (b_3) of the excited state of the radical (D_n) itself can only increase with oxygen, the lifetime of D_n has to decrease with oxygen. The quenching of D_n by oxygen seems unlikely because D_n should have a very short lifetime (it is expected to relax quickly by internal conversion), unless oxygen forms a complex with the dark state, in which case the reaction with oxygen is not diffusion-limited. Because we have no means of experimentally testing the quenching pathway of the excited radical, this scheme remains mere speculation. More intermediates might be involved.

Photobleaching and Temperature. The main decrease in photobleaching efficiency with temperature takes place between 295 and 200 K (cf. Figure 2c), in agreement with earlier observations that water plays an important role in photobleaching.[22,29,40] That photobleaching remains significant at 10 K shows that at least some bleaching processes have no activation barrier or very low ones. Possible candidates are the hydrogenation of the dye by a proton that tunnels from the matrix or electron transfer from or to a nearby donor site. Hydrogenated intermediates have been observed at low temperature in a fluorescence study of pentacene.[47]

Photobleaching of Single Molecules. Our single-molecule study is intended to be a qualitative comparison of the ensemble results. At room temperature, the histograms of the observed bleaching times in the single-molecule experiments (excitation intensity 1.5 kW/cm^2), can be fit with a single bleaching time (cf. Figure 5a and b) of 11 s in air and 22 s in the inert atmosphere. Although both histograms are clearly not single-exponential, the fit provides us with an average bleaching time. Both average bleaching times are considerably longer than those observed in the ensemble experiments at 320 W/cm^2 (cf. lower plots in Figure 2a). Furthermore, the bleaching times of the single molecules are shorter in air, in contrast to those of the bulk (cf. Figure 2a). The longer bleaching times indicate that the single molecules constitute a relatively bleaching-resistant subpopulation. These molecules contribute to the ensemble curves of Figure 2b mainly in the region after 10 s. (The intensity in the single-molecule experiments is 5 times higher.) As has been pointed out previously, these molecules bleach faster in air than in the inert atmosphere, in agreement with the single-molecule observations. The reduction factors of photobleaching efficiency on going from air to the inert atmosphere, 1.5 for the ensemble curves (between 30 and 100 s) and 2 for the single-molecule experiments, are in reasonable agreement. In the inert atmosphere, more molecules bleach at low illumination doses. This is expected to lead to lower numbers of detectable molecules, but we have not tested this experimentally.

The average bleaching time in air at 1.5 kW/cm^2, 11 s, agrees well with times reported earlier for similar excitation conditions. Mei et al.[15] report 15 s for R6G in trehalose at roughly 1 kW/cm^2, Hou et al.[22] report 12 s for nile red in PVA at approximately 1 kW/cm^2, and Hernando et al.[48] report 11 s for tetramethylrhodamine-5-isothiocyanate in PVA at 4.5 kW/cm^2. For the data in nitrogen, no direct comparison is available, but for systems with the triplet as the only dark state, the reduction in bleaching efficiency relative to that in air is at least 1 to 2 orders of magnitude.[10,21,31,32] Therefore, the observed reduction by a factor of 2 excludes the fact that the single molecules are those with the triplet as the only dark state. The smaller factor of 2 probably stems from secondary photobleaching of the radical anion in the inert atmosphere (cf. discussion of the ensemble experiments). The reduction of photobleaching is so small that it is doubtful whether removing oxygen is any help at all in detecting single molecules. We expect more resolvable molecules in air (cf. previous paragraph) and shorter off times in photoblinking.[41]

At 1.5 K, the histogram of the bleaching times reveals a very broad distribution (cf. Figure 5c) in which one-third of the molecules survive longer than 1000 s. In the ensemble experiment at 10 K (cf. Figure 2b), performed at a comparable intensity (320 W/cm^2 in the ensemble versus 400 W/cm^2 in the single-molecule experiment), 25% of the molecules live longer than 1000 s. This suggests that, as compared to the situation at room temperature, a larger fraction of molecules are observed as single molecules at low temperatures. This is not hard proof, however, because we might still look at a subpopulation with the same distribution of bleaching times as that of the total population. Further studies at variable temperatures are necessary to compare the number of discernible single molecules at low temperature and at room temperature.

Photoblinking of Single Molecules. Regarding photoblinking, it is interesting to investigate how the slow recovery rate from the radical anion D (with median values from 4 s^{-1} in air

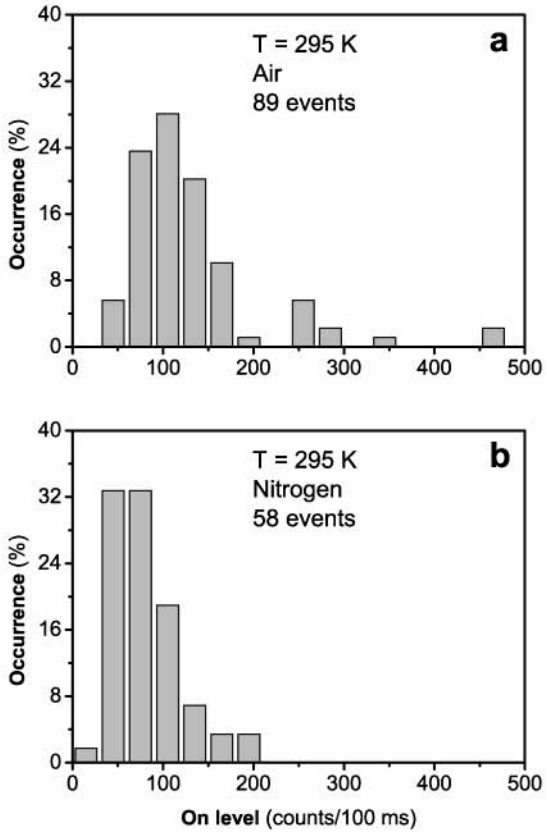

Figure 7. Histograms of the average on levels of the fluorescence time traces recorded in (a) air and (b) nitrogen at room temperature. The applied excitation intensity in the experiments was 1.5 kW/cm^2.

at 295 K to 0.2 s^{-1} below 80 K,[41] cf. Appendix) manifests itself at the single-molecule level. In principle, there are two extreme possibilities: there could be "bright" and "dark" molecules corresponding to short and long recovery times of their dark states, respectively, or each molecule could present both short and long dark periods in its fluorescence. In the first case, only the bright molecules will appear in a single-molecule experiment, and their fluorescence time traces will present only relatively short off times. The second case resembles the photoblinking of semiconductor nanocrystals,[49,50] where long and short off times are found in the fluorescence time trace of each individual nanocrystal. The fluorescence time traces of single R6G molecules in PVA (cf. Figure 4) only occasionally reveal photoblinking with off times longer than our time resolution of 100 ms, sometimes up to tens of seconds (cf. Figure 4b). Such long off times have also been observed for tetramethylrhodamine-5-isothiocyanate in PVA by Hernando et al.[48] and for R6G in poly(methyl methacrylate) by Vargas et al.[51] However, because most time traces do not display such long off times, single molecules seem brighter than the "average" molecule observed in the ensemble experiments. This suggests that photoblinking mainly leads to the existence of bright and dark molecules (i.e., it reduces the number of observable single molecules).

Off times shorter than 100 ms, our time resolution, can be probed by comparing the on levels between air and the inert atmosphere. An effect is expected because the recovery from D (and also from the triplet) is accelerated by oxygen.[41] Figure 7 shows histograms of the average on levels in air and nitrogen atmospheres at room temperature. The brightness is approximately 1.5 times lower in the inert atmosphere than in air, which confirms the fact that the off times are indeed on average longer in the inert atmosphere. If the photoblinking were completely related to the triplet, then a ratio of 3 would be expected between the average on levels in air and the inert atmosphere at 1.5 kW/cm^2. (This number can be calculated by taking the ratio of the steady-state emissivities (eq 2 in the Appendix) with the appropriate parameters for the triplet of R6G (cf. Appendix) in air and in the inert atmosphere.)

Although the radical anion as an additional dark state drastically alters the photophysics and photochemistry of R6G molecules in PVA, its effect on the observed single molecules does not seem that strong. We attribute this to the bias toward "bright" and stable molecules in the single-molecule experiments. Nevertheless, some differences remain with molecules that have the triplet as their only dark state. Long-off-time blinking events appear occasionally, and the reduction in the photobleaching quantum yield between air and the inert atmosphere is only a factor of 2, whereas it is 1 or 2 orders of magnitude for molecules with only a triplet dark state.[10,21,31,32]

Conclusions

We have studied the photobleaching of R6G in PVA on large ensembles of molecules with continuous-wave excitation. We have simulated our results with a kinetic model involving the triplet of R6G, the radical anion, and their excited states. We have distinguished four different photobleaching processes, all of them with nonexponential kinetics. Oxygen has been shown to play a double-sided role in the photobleaching. On one hand it stimulates bleaching by reacting with the metastable states, but on the other hand it reduces bleaching by shortening their lifetimes. This explains the counterintuitive observation that the main part of the ensemble bleaches faster in the inert atmosphere than in air at higher intensities. The small, bleaching-resistant part of the population, seen as single molecules, is only marginally more stable in the inert atmosphere. Photobleaching decreases significantly at low temperatures but does not vanish altogether. The results of the single-molecule experiments are in good agreement with the ensemble results. Photoblinking and photobleaching appear to reduce the number of observable single molecules rather than to shorten their observation times.

Our study demonstrates once more how complex photobleaching is. Although our findings strictly apply to R6G in PVA, we believe that some of them, such as the double role of oxygen and the occurrence of photobleaching processes with very low activation barriers, are of general value. The matrix PVA may also favor long-lived radical ion intermediates for other fluorophores and for labeled biomolecules.

Acknowledgment. We thank Jennifer Mathies, Elsbeth van der Togt, and Aurélien Nicolet for their contributions to the experiments and acknowledge helpful discussions with Professor E. J. J. Groenen. This work is part of the research program of the Stichting voor Fundamenteel Onderzoek der Materie (FOM) and is financially supported by the Nederlandse Organisatie voor Wetenschappelijk Onderzoek (NWO). We acknowledge support from the European Commission with a Marie Curie Fellowship for F.K. (contract no. HPMF-CT-2001-01233) and a postdoctoral fellowship within the project CHIC (contract no. IST-2001-33578) for M.A.K.

Appendix

The starting point of the derivation of the expression for the photobleaching decay is the steady-state emissivity before the onset of photobleaching.[41] For population 1, this steady-state

emissivity A_{4LS} reads as

$$A_{4LS}(I) = \frac{\sigma N \eta}{f}\left(1 + \frac{s}{f}\left(1 + \frac{d}{c}\right)\right)^{-1} \quad (2)$$

with s being the pump rate of the S_0-S_1 transition:

$$s = \sigma N I \quad (3)$$

σ is the absorption cross section of R6G in PVA at 514.5 nm (3.0×10^{-16} cm^2 [41]), N is the number of photons in 1 W at 514.5 nm (2.59×10^{18} photons/s), I is the absolute excitation intensity (W/cm^2), η is the fluorescence quantum yield of R6G (drops out eventually in the normalization of the emissivity), and f is the fluorescence rate of R6G (2.5×10^8 s^{-1} [44]). The pump rates s_D of the D_0-D_n and s_T of the T_0-T_n transitions (cf. Figure 6) obey equations similar to eq 3 with σ replaced by σ_D and σ_T, respectively, the (unknown) absorption cross sections of these transitions at 514.5 nm. For population 2, the expression of the steady-state emissivity, A_{3LS}, looks the same as eq 2 with c replaced by r. The intersystem crossing rate d of R6G is approximately 1.0×10^6 s^{-1} [41,44,45] (independent of temperature and atmosphere); the triplet recovery rate r is roughly 2.5×10^5 s^{-1} in air[46] and 2.5×10^3 s^{-1} in the inert atmosphere[44] (independent of temperature). The recovery rate from the radical anion (D), c, has been found to be distributed.[41] To provide an estimate of the magnitude of c, we give the median values of the obtained distributions: 4 s^{-1} in air at 295 K, 0.4 s^{-1} in the inert atmosphere at 295 K, and 0.2 s^{-1} in the inert atmosphere below 80 K. (The median of a distribution is the value of the distributed parameter at which one-half of the total integral of the distribution can be found at higher values and the other half can be found at lower values.)

The general expression for the emissivity decay due to photobleaching, Ω, is found by considering the bleached state to be an extra level (as indicated in Figure 6) and applying the steady-state approximation to the rate equations associated with all other levels. We neglect d and all bleaching rates with respect to f. For population 1, we obtain Ω_{4LS},

$$\Omega_{4LS}(I, t) = A_{4LS}(I) \exp(-\omega_{4LS}(I)t) \quad (4)$$

with a total bleaching rate ω_{4LS},

$$\omega_{4LS}(I) = P_{4LS}(I)\,(X_1 + IY_1) \quad (5)$$

with saturation parameter P_{4LS},

$$P_{4LS}(I) = \frac{s}{f}\left(1 + \frac{s}{f}\left(1 + \frac{d}{c}\right)\right)^{-1} \quad (6)$$

and with the effective bleaching parameters X_1 and Y_1,

$$X_1 = \frac{d}{q}b_1 + \frac{d}{c}b_2 \quad (7)$$

$$Y_1 = \frac{d}{c}\left(\frac{\sigma_D N}{j_D}\right)b_3 \quad (8)$$

For population 2, similar equations can be derived. The emissivity decay Ω_{3LS} has the same form as eq 4 with A_{4LS} and ω_{4LS} replaced by A_{3LS} and ω_{3LS}. The total bleaching rate ω_{3LS} equals

$$\omega_{3LS}(I) = P_{3LS}(I)\,(X_2 + IY_2) \quad (9)$$

with the saturation parameter P_{3LS} resembling eq 6 with c replaced by r, and the effective bleaching parameters X_2 and Y_2:

$$X_2 = \frac{d}{r}b_1 \quad (10)$$

$$Y_2 = \frac{d}{r}\left(\frac{\sigma_T N}{j_T}\right)b_4 \quad (11)$$

To reproduce the photobleaching decay traces, we need the total emissivity decay normalized to the emissivity at intensity $I_0 = 65$ mW/cm^2. At this intensity, no photobleaching is observed on a timescale of hours so that we effectively normalize to the steady-state emissivity related to photoblinking at this intensity. The normalized total emissivity decay due to photobleaching, Ω', then reads as

$$\Omega'(I, t) = \frac{0.95\Omega_{4LS}(I, t) + 0.05\Omega_{3LS}(I, t)}{0.95A_{4LS}(I_0) + 0.05A_{3LS}(I_0)} \quad (12)$$

Simulations are carried out for three distinct experimental conditions: air at 295 K, the inert atmosphere at 295 K, and the inert atmosphere at 10 K. The effective bleaching parameters X_1 (7), Y_1 (8), X_2 (10), and Y_2 (11) are used as fit parameters. When just the distribution of c[41] is taken into account, it is impossible to satisfactorily reproduce the experimental data (simulations not shown). Therefore the effective bleaching parameters are all allowed to be distributed and to change with the atmosphere and temperature. The distributions are supposed to be uniform and broad on a logarithmic scale. We approximate this by the following summation:

$$\langle f(k)\rangle = \frac{1}{N}\sum_{i=1}^{N} f(k_i) \quad (13)$$

where $\langle f(k)\rangle$ is the average over individual functions $f(k_i)$ of k_i, which are elements of the distribution of k. The elements k_i obey

$$k_i = \exp\left(\ln(C_k) + \frac{1}{N}\ln(W_k)\left(i - \frac{N+1}{2}\right)\right) \quad (14)$$

with C_k the central value and W_k the width of the distribution of parameter k. Reasonable accuracy is obtained when N is chosen equal to 10.

Two kinds of simulations are performed. First, only X_1 and X_2 are used as fit parameters to reproduce the data. We suppose that the value of X_2 is approximately 300 s^{-1} in air because the bleaching quantum yield of R6G in ethanol is known to be roughly 10^{-6}.[43] Furthermore, X_2 is expected to be at least 1 order of magnitude lower in the inert atmosphere.[10,21,31,32] The results are shown in Figure 1. For all three conditions, it is possible to fit the data at the lowest intensity. However, a direct extrapolation to higher intensities is feasible with the obtained parameters only for air at 295 K (cf. Figure 1a).

The data in the inert atmosphere can be fit only by including Y_1 and Y_2 (cf. Figure 1b and c). For air (cf. Figure 1a), the inclusion of Y_1 and Y_2 is also investigated. We suppose Y_2 to be reduced by a factor of 100 because of the change in the triplet lifetime. The introduction of Y_1 and Y_2 affects only the trace at 320 W/cm^2 but does not really improve the fit. Better fits might be obtained with distributions other than the uniform distribution in logarithmic space (eq 13).

Table 1 reports the values of X_1, Y_1, X_2, and Y_2 used in the simulations shown in Figure 1. All parameters are distributed.

TABLE 1

conditions	X_1 (s^{-1}) [width]	Y_1 (cm^2/J) [width]	X_2 (s^{-1}) [width]	Y_2 (cm^2/J) [width]
air 295 K	300 [10^3]	0.1 [10^2]	300 [10^2]	300×10^{-2} [10^3]
inert 295 K (1)	500 [10^2]		3 [10^2]	
inert 295 K (2)	50 [10^4]	50 [10^2]	3 [10^2]	3 [10^3]
inert 10 K	5 [10^4]	0.5 [10^2]	0.3 [10^3]	4×10^{-3} [10^6]

The width of the respective distribution is indicated between square brackets after each number, which itself gives the central value of the distribution on a logarithmic scale (cf. eqs 13 and 14). The data in the inert atmosphere at 295 K require secondary bleaching processes (Y_1 and Y_2) and a change of the primary bleaching parameter X_1. Both sets of parameters are given in Table 1.

References and Notes

(1) Funatsu, T.; Harada, Y.; Tokunaga, M.; Saito, K.; Yanagida, T. *Nature* **1995**, *374*, 555.

(2) Sase, I.; Miyata, H.; Corrie, J. E. T.; Craik, J. S.; Kinosita, K. *Biophys. J.* **1995**, *69*, 323.

(3) Schmidt, T.; Schütz, G. J.; Baumgartner, W.; Gruber, H. J.; Schindler, H. *J. Phys. Chem.* **1995**, *99*, 17662.

(4) Dickson, R. M.; Norris, D. J.; Tzeng, Y. L.; Moerner, W. E. *Science* **1996**, *274*, 966.

(5) Wennmalm, S.; Edman, L.; Rigler, R. *Proc. Natl. Acad. Sci. U.S.A.* **1997**, *94*, 10641.

(6) Weiss, S. *Science* **1999**, *283*, 1676.

(7) Schwille, P.; Haupts, U.; Maiti, S.; Webb, W. W. *Biophys. J.* **1999**, *77*, 2251.

(8) Zhuang, X. W.; Bartley, L. E.; Babcock, H. P.; Russell, R.; Ha, T. J.; Herschlag, D.; Chu, S. *Science* **2000**, *288*, 2048.

(9) Xie, X. S. *J. Chem. Phys.* **2002**, *117*, 11024.

(10) Yildiz, A.; Forkey, J. N.; McKinney, S. A.; Ha, T.; Goldman, Y. E.; Selvin, P. R. *Science* **2003**, *300*, 2061.

(11) Bruchez, M.; Moronne, M.; Gin, P.; Weiss, S.; Alivisatos, A. P. *Science* **1998**, *281*, 2013.

(12) Dahan, M.; Lévi, S.; Luccardini, C.; Rostaing, P.; Riveau, B.; Triller, A. *Science* **2003**, *302*, 442.

(13) Moerner, W. E. *J. Chem. Phys.* **2002**, *117*, 10925.

(14) van Oijen, A. M.; Ketelaars, M.; Köhler, J.; Aartsma, T. J.; Schmidt, J. *Science* **1999**, *285*, 400.

(15) Mei, E.; Tang, J. Y.; Vanderkooi, J. M.; Hochstrasser, R. M. *J. Am. Chem. Soc.* **2003**, *125*, 2730.

(16) Radford, S. E. *Trends Biochem. Sci.* **2000**, *25*, 611.

(17) Ha, T.; Xu, J. *Phys. Rev. Lett.* **2003**, *90*, 223002.

(18) Christ, T.; Kulzer, F.; Bordat, P.; Basché, T. *Angew. Chem., Int. Ed.* **2001**, *40*, 4192.

(19) Osborne, M. A.; Furey, W. S.; Klenerman, D.; Balasubramanian, S. *Anal. Chem.* **2000**, *72*, 3678.

(20) Göhde, W.; Fischer, U. C.; Fuchs, H.; Tittel, J.; Basché, T.; Bräuchle, C.; Herrmann, A.; Müllen, K. *J. Phys. Chem. A* **1998**, *102*, 9109.

(21) Hübner, C. G.; Renn, A.; Renge, I.; Wild, U. P. *J. Chem. Phys.* **2001**, *115*, 9619.

(22) Hou, Y. W.; Higgins, D. A. *J. Phys. Chem. B* **2002**, *106*, 10306.

(23) Song, L. L.; Hennink, E. J.; Young, I. T.; Tanke, H. J. *Biophys. J.* **1995**, *68*, 2588.

(24) Song, L. L.; Varma, C. A. G. O.; Verhoeven, J. W.; Tanke, H. J. *Biophys. J.* **1996**, *70*, 2959.

(25) Song, L. L.; van Gijlswijk, R. P. M.; Young, I. T.; Tanke, H. J. *Cytometry* **1997**, *27*, 213.

(26) Talhavini, M.; Atvars, T. D. Z. *J. Photochem. Photobiol., A* **1998**, *114*, 65.

(27) Talhavini, M.; Atvars, T. D. Z. *J. Photochem. Photobiol., A* **1999**, *120*, 141.

(28) Talhavini, M.; Corradini, W.; Atvars, T. D. Z. *J. Photochem. Photobiol., A* **2001**, *139*, 187.

(29) Hou, Y. W.; Bardo, A. M.; Martinez, C.; Higgins, D. A. *J. Phys. Chem. B* **2000**, *104*, 212.

(30) Dibbernbrunelli, D.; Deoliveira, M. G.; Atvars, T. D. Z. *J. Photochem. Photobiol., A* **1995**, *85*, 285.

(31) Weston, K. D.; Carson, P. J.; DeAro, J. A.; Buratto, S. K. *Chem. Phys. Lett.* **1999**, *308*, 58.

(32) English, D. S.; Furube, A.; Barbara, P. F. *Chem. Phys. Lett.* **2000**, *324*, 15.

(33) Eggeling, C.; Widengren, J.; Rigler, R.; Seidel, C. A. M. *Anal. Chem.* **1998**, *70*, 2651.

(34) Eggeling, C.; Widengren, J.; Rigler, R.; Seidel, C. A. M. In *Applied Fluorescence in Chemistry, Biology and Medicine*; Rettig, W., Strehmel, B., Schrader, S., Eds.; Springer-Verlag: Berlin, 1998.

(35) Somasundaram, G.; Ramalingam, A. *J. Photochem. Photobiol., A* **1999**, *125*, 93.

(36) Dittrich, P. S.; Schwille, P. *Appl. Phys. B* **2001**, *73*, 829.

(37) Chirico, G.; Cannone, F.; Baldini, G.; Diaspro, A. *Biophys. J.* **2003**, *84*, 588.

(38) van Dijk, M. A.; Kapitein, L. C.; van Mameren, J.; Schmidt, C. F.; Peterman, E. J. G. Submitted to *J. Phys. Chem. B.*

(39) Fleury, L.; Segura, J. M.; Zumofen, G.; Hecht, B.; Wild, U. P. *Phys. Rev. Lett.* **2000**, *84*, 1148.

(40) Dräbenstedt, A. Hochauflösende Spektroskopie und Mikroskopie Einzelner Molekule und Farbzentren Bei Tiefen Temperaturen. Ph.D. Thesis, Technical University of Chemnitz, Chemnitz, Germany, 1999, http://www.tu-chemnitz.de/physik/ARCHIV/PROMOT/.

(41) Zondervan, R.; Kulzer, F.; Orlinskii, S. B.; Orrit, M. *J. Phys. Chem. A* **2003**, *107*, 6770.

(42) van Oijen, A. M.; Köhler, J.; Schmidt, J.; Müller, M.; Brakenhoff, G. J. *J. Opt. Soc. Am. A* **1999**, *16*, 909.

(43) Barnes, M. D.; Whitten, W. B.; Ramsey, J. M. *Anal. Chem.* **1995**, *67*, A418.

(44) Dempster, D. N.; Morrow, T.; Quinn, M. F. *J. Photochem.* **1973/1974**, *2*, 343.

(45) Korobov, V. E.; Chibisov, A. K. *J. Photochem.* **1978**, *9*, 411.

(46) Nie, S. M.; Chiu, D. T.; Zare, R. N. *Science* **1994**, *266*, 1018.

(47) Astilean, S.; Corval, A.; Casalegno, R.; Trommsdorff, H. P. *J. Lumin.* **1994**, *58*, 275.

(48) Hernando, J.; van der Schaaf, M.; van Dijk, E. M. H. P.; Sauer, M.; Garcia-Parajó, M. F.; van Hulst, N. F. *J. Phys. Chem. A* **2003**, *107*, 43.

(49) Messin, G.; Hermier, J. P.; Giacobino, E.; Desbiolles, P.; Dahan, M. *Opt. Lett.* **2001**, *26*, 1891.

(50) Verberk, R.; van Oijen, A. M.; Orrit, M. *Phys. Rev. B* **2002**, *66*, 233202.

(51) Vargas, F.; Hollricher, O.; Marti, O.; de Schaetzen, G.; Tarrach, G. *J. Chem. Phys.* **2002**, *117*, 866.